

Measurement and analysis of excitation functions for alpha induced reactions on iodine and cesium

N P M SATHIK, M AFZAL ANSARI*, B P SINGH and R PRASAD

Department of Physics, Aligarh Muslim University, Aligarh 202 002, India

*Present address: Department of Physics, Garyounis University, Benghazi, Libya

MS received 18 March 1996; revised 8 July 1996

Abstract. The excitation functions for the reactions $^{127}\text{I}(\alpha, 2n)^{129}\text{Cs}$, $^{127}\text{I}(\alpha, 4n)^{127}\text{Cs}$, $^{133}\text{Cs}(\alpha, 2n)^{135}\text{La}$ and $^{133}\text{Cs}(\alpha, 4n)^{133}\text{La}$ have been measured up to ≈ 50 MeV α -particle energy using the stacked foil activation technique. Measured excitation functions are compared with pre-equilibrium geometry dependent hybrid model calculations. It has been found that theoretical calculations using an initial exciton number $n_0 = 4(2p + 2n + 0h)$ give good agreement with experimental excitation functions.

Keywords. α -induced reaction on I and Cs; stacked foil activation technique; $E_\alpha \leq 50$ MeV.

PACS No. 25-60

1. Introduction

Nuclear reactions induced by intermediate energy α -particles have been a point of interest during the last decade. The highly excited nuclear system, produced by projectile bombardment decays first by emitting a number of fast nucleons or clusters of nucleons at the pre-equilibrium (PE) stage and later on by evaporating low energy nucleons at the equilibrium (EQ) stage. The high energy tail observed in the experimental excitation functions may be explained through the PE emission process. Many semiclassical models [1–5] have been proposed to explain the features of the experimental excitation functions. Among these, the geometry dependent hybrid (GDH) model proposed by Blann [4] has been found to give a satisfactory reproduction of the experimental data. Efforts have been made to develop a fully quantum mechanical (QM) picture of PE reaction in the framework of multistep theories [6–10]. However, on account of the complexity involved in computation, the theoretical calculations for four nucleon systems like α -particle have not been found to give satisfactory results. The work presented here is a part of the programme of precise measurement of excitation functions for α -induced reactions, currently under way [11–19]. We report on the measurement of excitation functions for the alpha induced reactions on ^{127}I and ^{133}Cs . These reactions are important from the point of view of CsI detector design.

2. Experimental details

Excitation functions for the reactions $^{127}\text{I}(\alpha, 2n)^{129}\text{Cs}$, $^{127}\text{I}(\alpha, 4n)^{127}\text{Cs}$, $^{133}\text{Cs}(\alpha, 2n)^{135}\text{La}$ and $^{133}\text{Cs}(\alpha, 4n)^{133}\text{La}$ up to ≈ 50 MeV have been measured using stacked foil

activation technique and Ge(Li) gamma-ray spectroscopy. The experiment was performed at the Variable Energy Cyclotron Centre (VECC), Calcutta. Spectroscopically pure (SPECPURE) cesium iodide sample was used as the target material. The purity of the material was better than 99.9%. Targets were made by vacuum evaporation of about 1 mg/cm² thick cesium iodide on an aluminium backing of thickness 6.75 mg/cm², placed over the masking plate. In the masking plate there were thirteen open squares of size 12 mm × 12 mm. Since, CsI is a hygroscopic compound, a thin Al layer of thickness 200 µg/cm² was further deposited by vacuum evaporation onto the upper surface of the prepared CsI target, so that the moisture may not affect the target surface. These targets were cut into pieces and glued on aluminium frames of size 30 mm × 30 mm having a circular hole of diameter 10 mm in the centre. Samples for irradiation were taken in the form of a stack of these targets. Aluminium foil of various thicknesses were used as energy degraders and were sandwiched between the target foils wherever required so as to get the desired α-particle energy incident on each foil. The energy of incident α-particle on each foil in the stack was calculated from the energy degradation of incident α-particle beam using the stopping power tables of Northcliffe and Schilling [20]. The stack consisting of thirteen such targets was irradiated with a 50 MeV α-particle beam. By using a tantalum collimator placed in front of the stack the diameter of the beam spot was adjusted to 8 mm. The stack was screwed at the centre of the flange and was electrically insulated from the beam line. During irradiation the stack was cooled by a specially designed assembly through which low conductivity water (LCW) circulated. The stack was exposed to the unanalyzed external beam from the 224 cm variable energy cyclotron of VECC, Calcutta. The collimated α-particle beam of ≈ 100 nA falling on the target stack was monitored by charge collection using a Faraday cup, kept behind the target stack and coupled to an ORTEC current integrator. In many experiments the incident alpha beam flux has also been independently obtained using the standard reactions ²⁷Al(α, 4p 5n)²²Na and ²⁷Al(α, 4p 3n)²⁴Na for which the cross-section are said to be very well known [21]. However, in the present measurements the average incident α-beam flux was obtained from the total charge collected in the Faraday cup. After irradiation the induced gamma activities in individual foils were recorded with the help of a pre-calibrated high resolution 100 cm³ ORTEC Ge(Li) detector (FWHM 2 keV at 1.33 MeV) coupled to a CANBERRA-88 multichannel analyzer. The dead time for counting was kept less than 10% by adjusting the sample detector separation in these measurements. Several spectra were recorded at suitable time intervals to enable the identification of the half-lives of various residual nuclei. Various gamma-rays from a calibrated ¹⁵²Eu source (half-life 13.33 years) were used for the efficiency and the energy calibration of the counting unit. The expression used for computing the experimentally measured cross-sections is taken from ref. [22]. The reaction cross-section σ(E) at a given energy E, was calculated using the expression

$$\sigma(E) = \frac{A\lambda \exp(\lambda t_2)}{N_0 \theta \Phi(G\varepsilon) K [1 - \exp(-\lambda t_1)] [1 - \exp(-\lambda t_3)]}$$

where $K = [1 - \exp(-\mu d)]/(\mu d)$ is the correction for self absorption of gamma rays in the sample of thickness d (gm/cm²) and of absorption coefficient μ (cm²/gm); A is the

Excitation functions for alpha induced reactions

area under photo peak, λ is the decay constant of the residual nucleus, t_1 , t_2 and t_3 are respectively the period of irradiation, time lapsed between the stop of irradiation and the start of counting and the counting period, N_0 is the number of target nuclei in the sample. Φ is the incident α -beam flux, (Ge) is the geometry dependent efficiency of the detecting unit and θ the branching ratio for the specific gamma ray.

The activation cross-section for a given reaction has been determined from the intensities of the various identified gamma rays arising from the same residual nuclei. The reported value is the weighted average cross-section corresponding to various identified γ -rays of sufficient intensity. The spectroscopic data used in the cross-section measurement are taken from the table of isotopes [23]. The threshold energy for various reactions involved, half-lives, gamma ray energies and their absolute intensities are given in table 1. A typical observed gamma ray spectrum of CsI irradiated by ≈ 50 MeV α -particles is shown in figure 1. As can be seen from figure 1, various peaks in the spectrum originate due to various residual nuclei produced through different reactions. The reactions were identified by the characteristic γ -rays produced by the residual nuclei. The γ -ray of energy 372 keV (30.8%) is emitted from the residual nuclei ^{129}Cs produced via $^{127}\text{I}(\alpha, 2n)$ reaction. Further, as seen from the observed spectrum (figure 1), the 372 keV γ -ray looks like a doublet. The area under photopeak of interest was obtained using the peak fitting program of the CANBERRA-88 multichannel analyzer and an uncertainty of about $< 10\%$ in the area of photopeak for 372 keV has

Table 1. Reactions, threshold energies, half-lives of residual nuclei, γ -ray energies and branching ratios of gamma-decay.

Reaction	Threshold energy (MeV)	Half life $T_{1/2}$	Gamma-ray energy (MeV)	Absolute gamma-ray intensity (%)
$^{127}\text{I}(\alpha, 2n)^{129}\text{Cs}$	15.6	1.34 d	0.177	0.27
			0.279	1.33
			0.318	2.46
			0.372	30.80
			0.412	22.50
			0.549	3.42
			0.589	0.61
$^{127}\text{I}(\alpha, 4n)^{127}\text{Cs}$	33.6	6.25 h	0.125	15.60
			0.321	1.24
			0.412	58.00
			0.462	4.20
			1.197	0.17
$^{133}\text{Cs}(\alpha, 2n)^{135}\text{La}$	15.6	19.48 h	0.481	1.54
			$^{133}\text{Cs}(\alpha, 4n)^{133}\text{La}$	33.4
			0.302	1.24
			0.565	0.51
			0.618	0.80
			0.622	0.49
			0.846	0.48

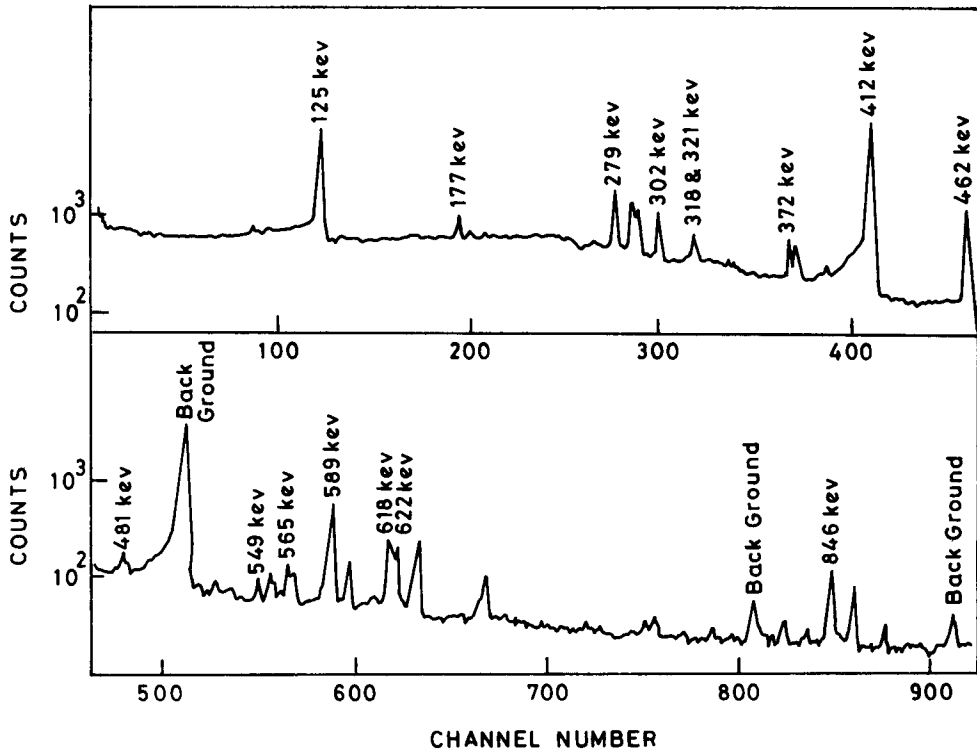


Figure 1. A typical gamma-ray spectrum of CsI irradiated by ≈ 50 MeV α -particle beam.

been obtained. As seen from table 1, the γ -ray of 412.0 keV is produced via two different reactions i.e., $^{127}\text{I}(\alpha, 2n)^{129}\text{Cs}$ and $^{127}\text{I}(\alpha, 4n)^{127}\text{Cs}$. Therefore, in the observed γ -ray spectrum beyond 33.6 MeV incident energy of alpha-particles (threshold for $(\alpha, 2n)$ reaction), the intensity of 412.0 keV γ -ray will have a contribution due to both these reaction channels. However, below 33.6 MeV the contribution will be due to $^{127}\text{I}(\alpha, 2n)^{129}\text{Cs}$ reaction only. In the present calculations the γ -ray of 412.0 keV is used for the measurement of cross-section of $(\alpha, 2n)$ reactions in ^{127}I up to ≈ 33 MeV only. As can be seen from table 1, the γ -ray of 549 keV (3.42%) and 589 keV (0.61%) are emitted from the residual nucleus ^{129}Cs produced in the $^{127}\text{I}(\alpha, 2n)$ reaction. Therefore, the intensity of 549 keV γ -ray should be stronger than the 589 keV γ -ray. However, from the observed spectrum (figure 1) it may be seen that the 589 keV γ -ray appears to be stronger than 549 keV γ -ray. The main reason for this anomaly may be that some interfering γ -rays, like $E_\gamma \approx 585$ keV (0.2%) from the residual nucleus ^{133}La produced in $^{133}\text{Cs}(\alpha, 4n)$, may be emitted which may contribute to the intensity of 589 keV γ -rays. As such the 589 keV γ -ray has not been used for computing the cross-section for $^{127}\text{I}(\alpha, 2n)^{129}\text{Cs}$ reaction. The presently measured cross-sections at different energies for the reactions $^{127}\text{I}(\alpha, 2n)^{129}\text{Cs}$, $^{127}\text{I}(\alpha, 4n)^{127}\text{Cs}$, $^{133}\text{Cs}(\alpha, 2n)^{135}\text{La}$ and $^{133}\text{Cs}(\alpha, 4n)^{133}\text{La}$ are tabulated in tables 2 and 3, along with the overall errors, including statistical errors of counting, expected due to various factors mentioned in §2.1.

Excitation functions for alpha induced reactions

Table 2. Measured cross-sections for α -induced reaction in ^{127}I .

$E_\alpha(\text{MeV})$	$^{127}\text{I}(\alpha, 2n)^{129}\text{Cs}$ Cross-section (mb)	$^{127}\text{I}(\alpha, 4n)^{127}\text{Cs}$ Cross-section (mb)
18.06 \pm 0.57	136.7 \pm 17.6	—
19.78 \pm 0.56	618.6 \pm 74.4	—
21.39 \pm 0.56	1040.6 \pm 123.9	—
24.26 \pm 0.56	1165.9 \pm 138.5	—
26.87 \pm 0.55	1214.7 \pm 144.2	—
30.37 \pm 0.55	1346.1 \pm 159.2	—
33.63 \pm 0.54	628.4 \pm 75.3	—
36.68 \pm 0.54	255.2 \pm 31.6	—
39.57 \pm 0.54	187.0 \pm 24.6	105.0 \pm 17.7
42.36 \pm 0.54	99.6 \pm 18.0	281.9 \pm 41.1
44.99 \pm 0.53	75.9 \pm 18.5	636.5 \pm 92.5
47.50 \pm 0.53	62.6 \pm 19.9	839.0 \pm 123.8
49.93 \pm 0.53	51.6 \pm 21.3	821.5 \pm 128.7

Table 3. Measured cross-sections for α -induced reaction in ^{133}Cs .

$E_\alpha(\text{MeV})$	$^{133}\text{Cs}(\alpha, 2n)^{135}\text{La}$ Cross-section (mb)	$^{133}\text{Cs}(\alpha, 4n)^{133}\text{La}$ Cross-section (mb)
18.06 \pm 0.57	118.7 \pm 17.7	—
19.78 \pm 0.56	545.1 \pm 70.3	—
21.39 \pm 0.56	961.3 \pm 120.0	—
24.26 \pm 0.56	1098.8 \pm 126.4	—
26.87 \pm 0.55	1154.8 \pm 133.5	—
30.37 \pm 0.55	500.1 \pm 57.8	—
33.63 \pm 0.54	259.3 \pm 37.1	—
36.68 \pm 0.54	241.9 \pm 34.5	—
39.57 \pm 0.54	173.9 \pm 28.8	288.4 \pm 43.8
42.36 \pm 0.54	107.9 \pm 25.6	457.0 \pm 68.9
44.99 \pm 0.53	125.9 \pm 41.2	1156.6 \pm 167.2
47.50 \pm 0.53	98.7 \pm 47.9	1684.4 \pm 240.7

2.1 Experimental errors

The uncertainties may arise in measured cross-sections due to the errors in the estimation of target nuclei in the sample, the variation of the beam current which results in uncertainty of the incident flux, the uncertainty in the detector efficiency determination due to the statistical errors of counting of standard source, the uncertainty due to the solid angle effect due to non-reproducibility of the identical geometries for the standard source and the irradiated samples, etc. The additional uncertainties in measured cross-sections may come up due to the nuclei recoiling out of the sample. In some cases where intensity of activities produced in the irradiated samples were large, the dead time of the detector may also introduce uncertainty in the measured cross-section. The low energy neutrons which are produced when the beam traverses the stack material may also disturb the yield.

Analyses for all the above mentioned factors, expected to introduce errors have been done. In order to estimate the uncertainty in the number of target nuclei and to check the thickness and uniformity of the sample, pieces of sample foils were weighed on an electronic microbalance and the thickness of each piece was calculated. The errors in the estimation of the number of target nuclei were analyzed in this way and were estimated to be $< 1\%$. The uncertainty due to flux variation is $< 4\%$. The uncertainty in the detector efficiency due to the statistical error of counting is estimated to be $< 1.5\%$. However, the uncertainty due to the solid angle effect, since the irradiated samples were not point sources, is estimated using the prescription given by Gardner and Verghese [24] and is found to be $< 5\%$. Therefore, the total uncertainty in the efficiency is estimated to be $< 6.5\%$. To avoid the uncertainty due to recoiling of the nuclei out of the sample, the targets were placed perpendicular to the incident alpha-beam such that CsI deposition faced the incident beam. As such, the recoiling nuclei are likely to be trapped in Al backing. Hence, no correction is applied for that. In order to minimize the errors due to the dead time, particularly for the cases where the activity in the irradiated samples were large, the sample-detector distance was suitably adjusted to keep the dead time $< 10\%$. However, the corrections were applied in the counting rates accordingly. Also, as the beam traverses the stack material, low energy neutrons may be released, which in turn may disturb the yield. However, Ernst *et al* [25] have indicated that such disturbing yields are also negligible.

The overall error due to all these factors, as mentioned above, is expected to be $< 12\%$. The errors mentioned in cross-section in tables 2 and 3 are the overall error including the statistical errors of counting and are generally $< 20\%$ except for a few points. These errors do not include the uncertainty of the nuclear data such as the branching ratio, decay constant, etc., which are taken from the table of isotopes and the nuclear data sheets.

3. Results and discussion

Presently measured excitation functions for the reactions $^{127}\text{I}(\alpha, 2n)^{129}\text{Cs}$ and $^{127}\text{I}(\alpha, 4n)^{127}\text{Cs}$ are shown in figure 2 and for reactions $^{133}\text{Cs}(\alpha, 2n)^{135}\text{La}$ and $^{133}\text{Cs}(\alpha, 4n)^{133}\text{La}$ are shown in figure 3 respectively. To the best of our knowledge no earlier measurement has been done in the above energy region for these reactions. In these figures dark as well as open circles represent the measured cross section. The horizontal bars are the α -particle energy spread within the target thickness along with the inherent uncertainty in the α -particle beam and vertical bars represent the overall uncertainty in the measured cross-sections.

A computer code ALICE/LIVERMORE-82 [26] has been used for calculating the excitation functions theoretically. This code is capable of performing the theoretical excitation function calculations up to an energy range of 200 MeV.

The theoretical calculations of the excitation functions has been done within the framework of Weisskopf–Ewing model [27] for CN calculations while the PE calculations are performed employing geometry dependent hybrid-model of Blann [4]. In the Weisskopf–Ewing formulation, the conservation of angular momentum is not taken into account explicitly. However, an approximate treatment of angular momentum effect is incorporated by using *s*-wave approximation [[28]. In the GDH model the

intranuclear transition rates may be evaluated both from the imaginary optical potential parameters of Becchetti and Greenlees [29] and from Pauli corrected nucleon-nucleon scattering cross-sections [30]. Both the above methods give similar results [31]. However, optical model parameter set is valid up to 55 MeV projectile energies. In the present calculations the latter option has been used. The nuclear masses were calculated from the Myers and Swiatecki Lysekil mass formula [32]. The mean free path (MFP) is required to calculate the intranuclear transition rates. As the calculated MFP for two-body residual interactions may differ from the actual MFP, an adjustable parameter COST is provided in the code to match the experimental and theoretical excitation functions. The theoretical calculations were performed using different values of the parameter COST and a value of 3 best fits the data. The initial configuration of the initially excited number of particles and holes, also referred to as initial exciton number n_0 is the starting point in any particle induced nuclear reaction. As such the initial exciton number n_0 is an important parameter of PE calculations. In the present calculations the initial exciton configuration $n_0 = 4$ (2 protons + 2 neutrons and no hole) for α -particle is taken.

The level density parameter is also an important parameter in these calculations. In this code the level density $a = (A/PLD)$ is taken, where A is the mass number and PLD is the level density parameter. Though, the default option for the PLD is 9, a value of $PLD = 10$ ($a = A/10$) is found to give satisfactory reproduction of the data. With the

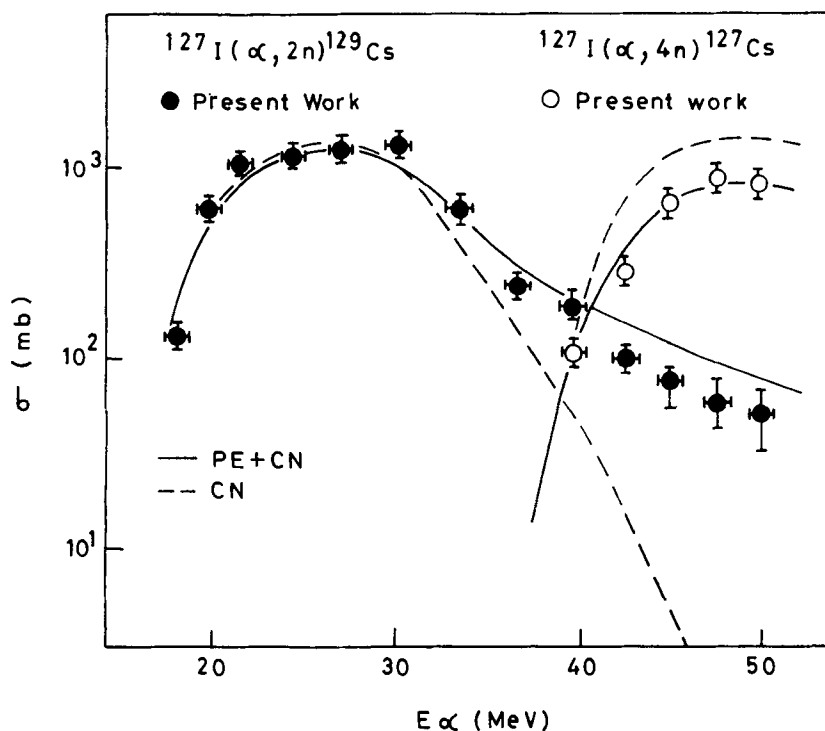


Figure 2. Experimentally measured and theoretically calculated excitation functions for $^{127}\text{I}(\alpha, 2n)^{129}\text{Cs}$ and $^{127}\text{I}(\alpha, 4n)^{127}\text{Cs}$ reactions.

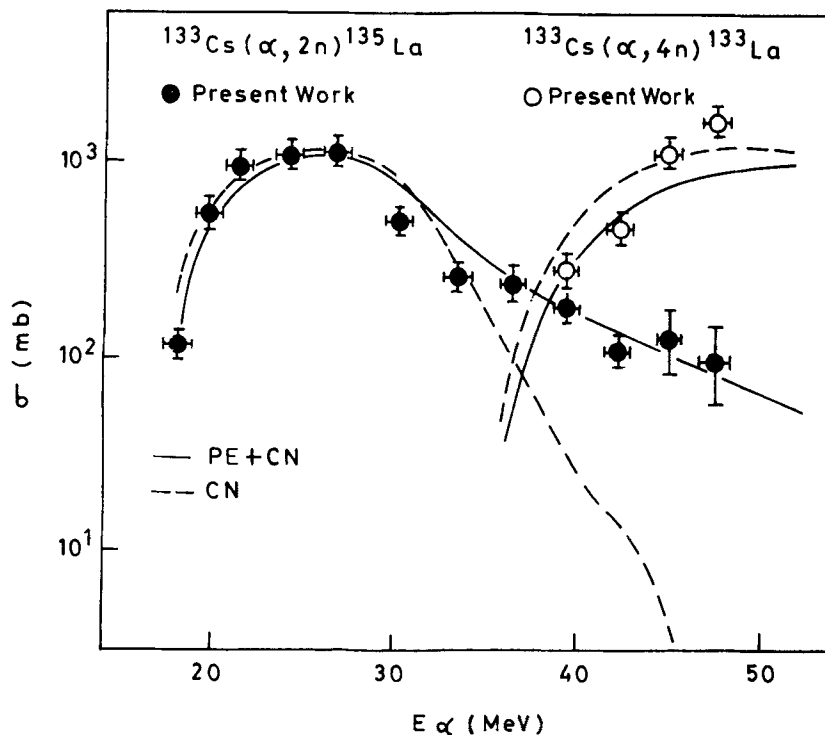


Figure 3. Experimentally measured and theoretically calculated excitation functions for $^{133}\text{Cs}(\alpha, 2n)^{135}\text{La}$ and $^{133}\text{Cs}(\alpha, 4n)^{133}\text{La}$ reactions.

choice of the appropriate set of these parameters the theoretical calculations have been performed. In the present calculations the initial exciton number $n_0 = 4(2p + 2n + 0h)$ along with the mean free path multiplier equal to 3 and the level density parameter $a = A/10$, have been found to give a satisfactory reproduction of the experimental data. In figures 2 and 3, the excitation functions are represented by solid curves for the calculations obtained by the consideration of both the CN and PE contributions while the broken line is for the CN (Weisskopf–Ewing) calculations. From figures 2 and 3, it may be observed that experimentally measured excitation functions, particularly the tail portions, cannot be reproduced by CN calculations only. However, proper admixture of equilibrium (CN) and PE contributions is needed to explain the excitation functions satisfactorily. In the present experiment, excitation functions for $^{127}\text{I}(\alpha, n)^{130}\text{Cs}$, $^{127}\text{I}(\alpha, 3n)^{128}\text{Cs}$, $^{133}\text{Cs}(\alpha, n)^{136}\text{La}$ and $^{133}\text{Cs}(\alpha, 3n)^{134}\text{La}$ reactions could not be measured due to short half-lives of the product nucleus. However, the residual nuclei produced in these reactions are also involved in the successive evaporation chain of the other reactions for which excitation function are measured presently.

4. Conclusions

From the above analysis it may be concluded that α -induced excitation functions have high energy tails, which in general cannot be accounted for by pure equilibrium

reaction mechanism. Proper admixture of equilibrium and PE processes is needed in theoretical calculations for better reproduction of experimentally measured excitation functions. It may also be inferred from these figures that for α -particle induced reactions the choice of initial exciton number $n_0 = 4$ with configuration (2 protons, 2 neutrons and no hole) gives satisfactory reproduction of the experimental data.

Acknowledgements

The authors would like to thank Prof M S Z Chaghtai, for providing necessary facilities to carry out this work. They are also thankful to VECC personnel for their help and co-operation during the course of this experimental work. One of the authors (NPMS) acknowledges the financial support in the form of University Research Fellowship awarded by AMU, Aligarh.

References

- [1] M Blann, *Ann. Rev. Nucl. Sci.* **25**, 123 (1975)
- [2] J J Griffin, *Phys. Rev. Lett.* **17**, 478 (1966)
- [3] E Gadioli, E Gadioli-Erba and P G Sona, *Nucl. Phys.* **A217**, 589 (1973)
- [4] M Blann, *Phys. Rev. Lett.* **27**, 337 (1971); **27**, 700 (1971); **27**, 1550 (1971)
- [5] G D Harp and J M Miller, *Phys. Rev.* **C3**, 1847 (1971)
- [6] H Feshbach, A Kerman and S Koonin, *Ann. Phys.* **125**, 429 (1980)
- [7] D Agassi, H A Weidenmueller and G Mantzouranis, *Phys. Rev.* **22**, 145 (1975)
- [8] T Tamura, T Udagawa, D H Feng and K K Kaur, *Phys. Lett.* **B68**, 109 (1977)
- [9] K W McVoy *et al*, *Phys. Rep.* **94**, 140 (1983)
- [10] H Gruppelaar *et al*, *La Rivista del Nuovo Cimento* **9**, 7 (1986)
- [11] H D Bhardwaj and R Prasad, *Nucl. Instrum. Methods* **A242**, 286 (1986)
- [12] I A Rizvi, M Afzal Ansari, R P Gautam, R K Y Singh and A K Chaubey, *J. Phys. Soc. Jpn.* **56**, 3135 (1987)
- [13] M Afzal Ansari, R K Y Singh, I A Rizvi, M K Bhardwaj and A K Chaubey, Internal Report IC/88/57 (ICTP, Trieste, 1988)
- [14] I A Rizvi, M K Bhardwaj, M Afzal Ansari and A K Chaubey, *Can. J. Phys.* **67**, 870 (1989)
- [15] H D Bhardwaj, A K Gautam and R Prasad, *Pramana – J. Phys.* **31**, 109 (1988)
- [16] B P Singh, M G V Sankaracharyulu, M Afzal Ansari, R Prasad and H D Bhardwaj, *Int. J. Mod. Phys.* **E1**, 823 (1992)
- [17] M Afzal Ansari, N P M Sathik, B P Singh, M G V Sankaracharyulu and R Prasad, Internal Report IC/94/299 (ICTP, Trieste, 1994)
- [18] B P Singh, M G V Sankaracharyulu, M Afzal Ansari, H D Bhardwaj and R Prasad, *Phys. Rev.* **47**, 2055 (1993)
- [19] N P M Sathik, M Afzal Ansari, B P Singh, M G V Sankaracharyulu and R Prasad, *Int. J. Mod. Phys.* **E5**, 345 (1996)
- [20] L C Northcliffe and R F Schilling, *Nucl. Data Tables* **A7**, 256 (1970)
- [21] R Michel and G Brinkmann, *Nucl. Phys.* **A338**, 167 (1980)
- [22] M Afzal Ansari, R K Y Singh, M Sehgal, V K Mittel and D K Avasthi, *Ann. Nucl. Energy* **11**, 173 (1984)
- [23] C M Lederer and V S Shirley, Table of isotopes, 7th edition (Wiley and Sons Inc., New York, 1978)
- [24] R P Gardner and K Verghese, *Nucl. Instrum. Methods* **93**, 163–167 (1971)
- [25] J Ernst, R Iowski, H Klampfl, H Machner, T Mayer-Kuckuk and R Schanz, *Z. Phys.* **A308**, 301 (1982)
- [26] M Blann and J Bisplinghoff, ALICE/LIVERMORE-82, Report UCID-19614 (1982)
- [27] V F Weisskopf and D H Ewing, *Phys. Rev.* **57**, 472 (1940)

- [28] T Ericson, *Adv. Phys.* **9**, 425 (1960)
- [29] F D Becchetti and G W Greenlees, *Phys. Rev.* **182**, 1190 (1969)
- [30] K Kikuchi and M Kawai, *Nuclear matter and nuclear interactions* (North-Holland, Amsterdam, 1968)
- [31] M Blann, *Nucl. Phys.* **A213**, 570 (1973)
- [32] W D Myers and W J Swiatecki, *Ark. Fys.* **36**, 343 (1967)